Effect of Electromagnetic Stirring on Weld Solidification Structure of Aluminum Alloys (Report II)†

–Investigation on GTA in DCSP Weld Metal of 8 mm Thick Plate –

Fukuhisa MATSUDA*, Kazuhiro NAKATA**, Yoshiaki MIYANAGA***,
Tetsuo KAYANO**** and Kenji TSUKAMOTO****

Abstract

In order to investigate the effect of the electromagnetic stirring of the molten metal on the grain refinement of the solidification structure and the eliminations of the feathery crystal and porosities, GTA in DCSP bead-on-plate welding was carried out for aluminum alloys of 5083-o, 5052-o and 1070-o of 8 mm thick plate as shielding gas of helium with electromagnetic stirring in the weld puddle during welding. Moreover, the application of the electromagnetic stirring to the actual welding process of square groove double butt welding with filler metal for 5083-o has been examined. Main conclusions obtained are as follows;

(1) There was the most effective frequency of alternate magnetic field for the grain refinement, that is, 2 to 15 Hz. The degree of the grain refinement decreased in higher or lower frequency than the optimum frequency. (2) An increase in intensity of the magnetic field was effective to the grain refinement, but there was an limit in the intensity of the magnetic field owing to the formation of a puckering weld bead. (3) The magnetic stirring was also effective to eliminating the formation of the feathery crystal and porosities. (4) The electromagnetic stirring remarkably increased the soundness of the butt welds of 5083-o with filler metal by suppressing the formation of the feathery crystal and large porosities and also refining the grains.

1. Introduction

As the method for the improvement of the weld solidification structure, several methods have been proposed and attempted, so for. Among these processes, it is considered that the electromagnetic stirring is one of the most effective methods and the applications of the electromagnetic stirring to the welding process have been attempted[1-9]. The authors also have attempted the electromagnetic stirring of the molten metal during the GTA bead-on-plate welding in dcrp for the thin sheet of the aluminum alloys and have widely investigated the effect of the electromagnetic stirring on the weld solidification structure[10]. As a result, it has been made clear that the electromagnetic stirring of the molten metal was very effective to the grain refinement and the suppression of the formation of the porosities and the feathery crystal.

On the other hand, recently the GTA welding in dcsp type with the shielding gas of helium (He) or a mixing gas of helium with argon (Ar) has begun to be used as one of the most excellent welding methods for the aluminum alloys[11] because of its deep penetrated weld bead. In this welding method, there are some problems that the elongated irregular porosities are very often formed especially in the butt welds because of the lack of the cleaning action and the feathery crystals are also often formed in some aluminum alloys such as 5083-o alloy. These problems decrease the soundness of the welded joint.

In the present work, in order to investigate the effect of the electromagnetic stirring of the molten metal on the weld solidification structure, the GTA bead-on-plate welding in dcsp type with He gas shielding without filler metal was performed for some aluminum alloys of about 8 mm thick plate. Then, the effects of the intensity and the frequency of the magnetic field on the grain refinement and the eliminations of the feathery crystal and the porosities have been investigated. Moreover, the electromagnetic stirring was applied on the GTA in dcsp square butt welding of two passes from top and back sides with filler metal with shielding gas of He. This welding process has been actually used for the welding of large components such as the LNG tank and then the effect of the electromagnetic stirring on the grain refinement and eliminations of the feathery crystal and porosites has also

† Received on October 2nd, 1978
* Professor
** Reseach associate
*** Graduate student
**** Showa Aluminum Co., Ltd.

been expected.

2. Materials Used and Experimental Procedure

2.1 Materials used

The materials used are mostly 5083-o Aluminum-Magnesuim-Manganese (Al-Mg-Mn) alloy and partly 5052-o Al-Mg and 1070-o commercially pure aluminum alloys. As a filler metal, 5183 (1.6 mmϕ) was used in the butt welding of 5083-o. The chemical compositions and plate thickness of these materials are listed in **Table 1**.

Table 1 Chemical compositions of materials used.

Material		Thickness (mm)	Chemical composition (wt.%)								
			Cu	Si	Fe	Mn	Mg	Zn	Cr	Ti	B
Base metal	1070-o	7.5	<0.01	0.05	0.13	<0.01	<0.01	0.01	–	0.004	<0.002
	5052-o	8.0	0.02	0.10	0.27	<0.01	2.36	0.01	0.19	0.009	<0.002
	5083-o	8.0	0.01	0.14	0.18	0.65	4.60	0.01	0.10	0.008	<0.002
Filler metal	5183	–	<0.01	0.07	0.16	0.67	5.00	<0.01	0.07	0.007	0.002

The dimensions of the materials used are 250 mm in length and 200 mm in width.

2.2 Experimental procedure

2.2.1 Electromagnetic stirring apparatus

The schematic illustration for the principle of the electromagnetic stirring in this investigation is shown in **Fig.1**. The molten metal in the weld pool is stirred by the

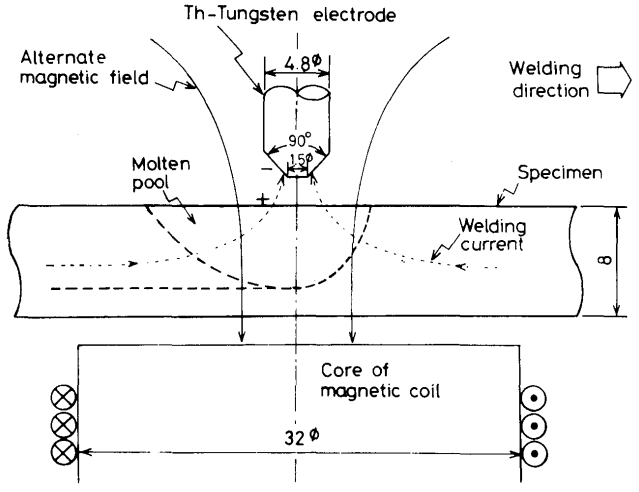

Fig. 1 Illustration of principle of electromagnetic stirring and arrangement of magnetic coil, welding torch and specimen

Lorentz force induced by the interaction of welding current passing through weld pool and the magnetic field perpendicular to the plate surface. In order to make an effective stirring of the molten metal an alternate square wave generator has been used for a power source of a magnetic coil, which can induce a continuous variation of the intensity and frequency of the magnetic field up to 800 G and from 0.1 to 100 Hz respectively. Arrangement of a magnetic coil, a welding torch and a specimen is also shown in Fig. 1. The magnetic coil was fixed in line with the center of the welding torch but under the specimen. The specimen can be moved in the preliminary setting speed by an automatic carriage. This arrangement essentially produces a vertical field in the arc and the weld zone.

2.2.2 Welding method

A GTA bead-on-plate welding in dcsp without filler metal has been carried out in a distance of 2 mm between the electrode and the specimen. He gas was usually used for a shielding gas and He +H_2 mixing gas with 0.5% H_2 was also used in order to examine the formation of the porosities. A flow rate of the shielding gas was 35 liters/min in all weldings. The welding speed was changed from 150 to 1000 mm/min and the optimum welding current for each test was selected such that the penetration depth was kept about 6 mm without the electromagnetic stirring.

Moreover, in butt welding, the full automatic welder has been applied, so that the arc voltage was kept to a constant value even during the electromagnetic stirring.

3. Experimental Results and Discussions

3.1 Weld solidification structure in weld metal of GTA welding in dcsp

It is well known that the mode of the macrostructure in the weld metal largely depends on the welding condition. Therefore, at first, the macrostructural change against the welding condition has been investigated in the weld metal of 5083-o.

The typical examples of the macrostructure observed in the GTA (dcsp) weld metal are shown in **Fig. 2**, where the three demensional mode of the macrostructure is shown. At the welding speed of 150 mm/min, the macrostructure consists of the columnar crystal, at 300 mm/min, the feathery crystal appeared in the central zone of the weld metal and more high welding speed of 750 mm/min, the equiaxed crystals became appeared in the central zone of the weld bead instead of the feathery crystal, although near the fusion boundary in the weld bead the columnar crystals are even observed.

Figure 3 shows the macrostructual changes against the welding conditions in the central zone of the weld bead.

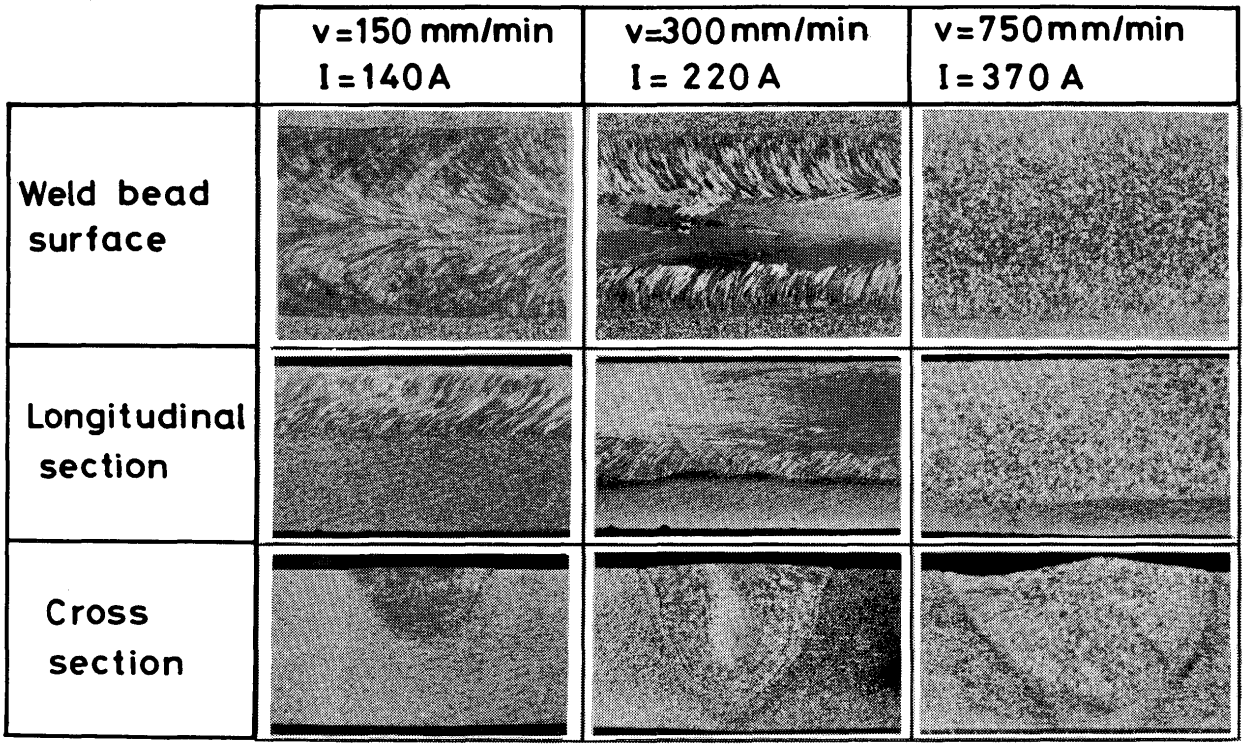

Fig. 2 Typical macrostructures of GTA (dcsp) weld metal of 5083-o

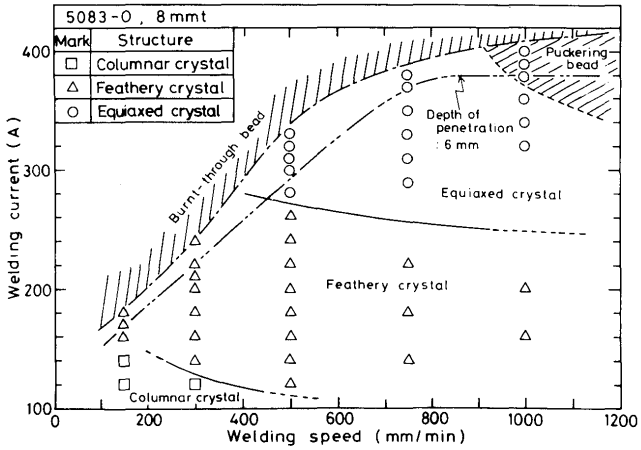

Fig. 3 Relation between welding condition and solidification structure in weld center.

In Fig. 3, the burnt-through weld bead was observed in the hatched zone. In the double hatched zone the puckering weld bead was mainly observed. As a result, it is apparent that the feathery crystal is inclined to be formed in the wide range of welding speed, that is, 150 to 1000 mm/min. The welding speed in the range of 150 to 1000 mm/min is mostly adopted in the actual welding process. Moreover, from a viewpoint of the mechanical properties of the weld metal, the formation of the feathery crystal should be avoided because it lowers the elongation of the welded joint[12].

3.2 Effect of electromagnetic stirring for grain refinement

3.2.1 Effective condition of electromagnetic stirring for grain refinement

The macrostructures of the weld metal at the top surface of the weld bead are shown in **Figs. 4(a)** and **(b)** for 5083-o and 5052-o, respectively, against the intensity and frequency of the magnetic field. The welding speed and the welding current are 300 mm/min and 220 amp, respectively. In Fig. 4(a) for 5083-o, it is apparent that there are optimum frequencies of the magnetic field, where the grain refinement is the most remarkable. This range of the optimum frequencies is considerably wide, that is, from 2 to 15 Hz which depended on the intensity. At the higher frequency, the effect of the electromagnetic stirring abruptly decreased. Next, as to the intensity of the magnetic field, the optimum intensities also exist where the grain refinement is the most remarkable and also the appearance of the weld bead surface is not so rough. For an example, at 5 Hz in a weak intensity such as 50 G, the effect of the magnetic stirring is small, so the feathery crystal is even observed. At the optimum intensity, that is, 100 G, the grain refinement is the most remarkable and the feathery crystal is not formed. Increasing the intensity more than 150 G, however, the surface of the weld bead became very rough such as that of the puckering weld bead and more than 300 G, the weld bead was burnt-through in every frequencies. As the

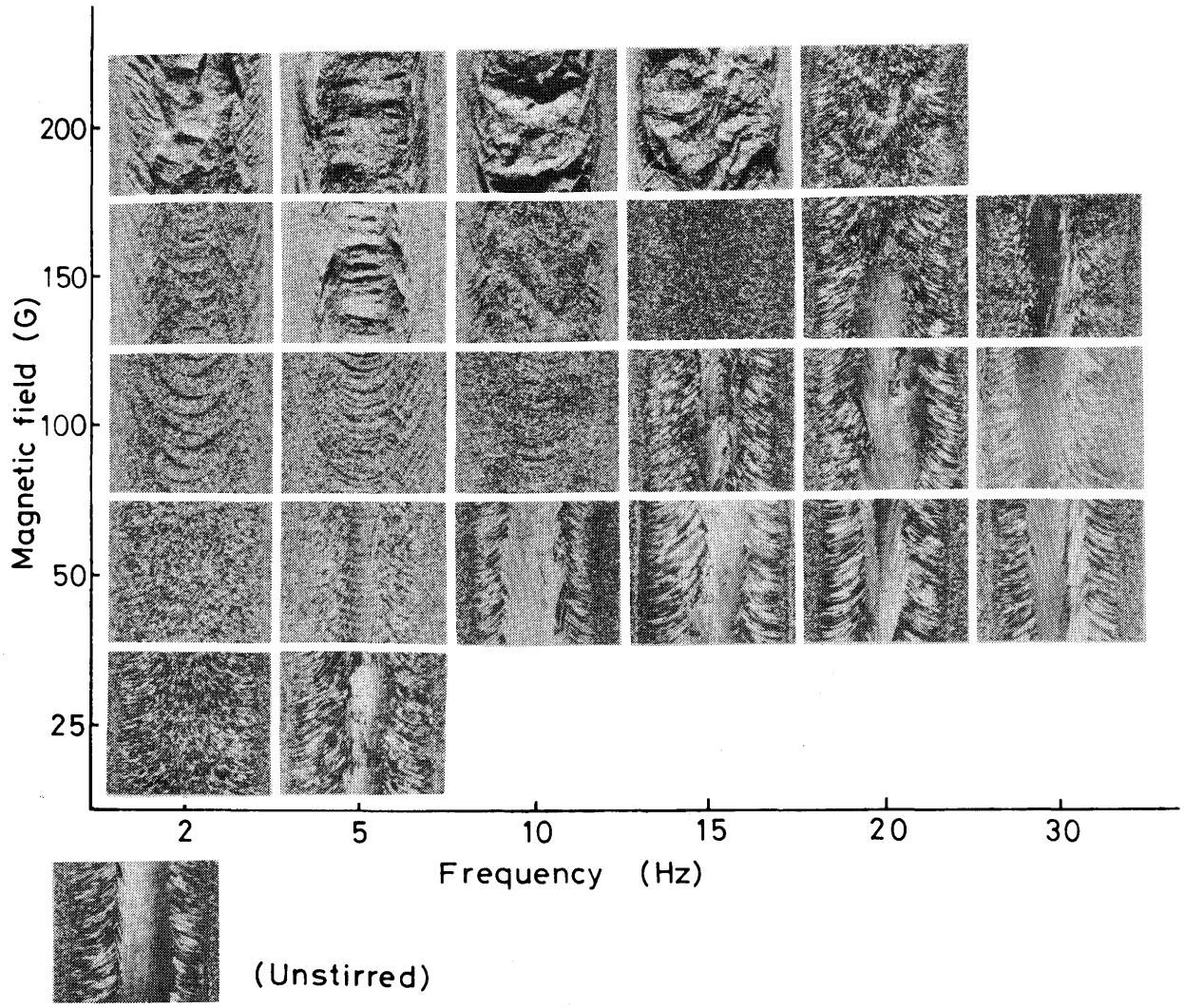

Fig. 4 (a) Macrostructures of 5083-o weld metals as functions of frequency and intensity of magnetic field: I=220 amp, V=300mm/min.

increase of the frequency to 15 Hz, the stronger intensity was needed for the grain refinement. As a conclusion, the optimum stirring conditions are as follows in this experiment for 5083-o 8 mm thick alloy, 100 to 150 G in 2 Hz, 100 G in 5 Hz, 100 G in 10 Hz and 150 G in 15 Hz.

In the case of 5052-o as shown in Fig. 4(b), the optimum range of the stirring condition for the grain refinement also existed but was restricted around 100 G, 5 Hz, which was much narrower than that for 5083-o. The degree of the grain refinement abruptly decreased at the lower or higher frequency than 5 Hz. On the contrary, the grain refinement has not been observed in the welds of 1070-o in any stirring condition in this investigation. Consequently, the materials used in this experiment were arranged as follows in order of the susceptibility for the grain refinement; 5083-o > 5052-o > 1070-o.

The grain refinement has been achieved not only at the top surface of the weld bead but also throughout the weld bead. **Figure 5** shows an typical example of the refined macrostructure at the top surface in **(a)** and the longitudinal crosssection in **(b)** for the weld bead of 5083-o. The grains are refined as the same way throughout the weld bead.

3.2.2 Microstructural change of weld solidification structure caused by electromagnetic stirring

Figure 6 shows the microstructure in the central zone in the 5052-o weld bead along the welding direction with the frequencies of 2 and 5 Hz under the same welding condition and magnetic field, that is, 300 mm/min of welding speed, 220 amp of welding current and 100 G of the intensity of the magnetic field. Each pair of the bold

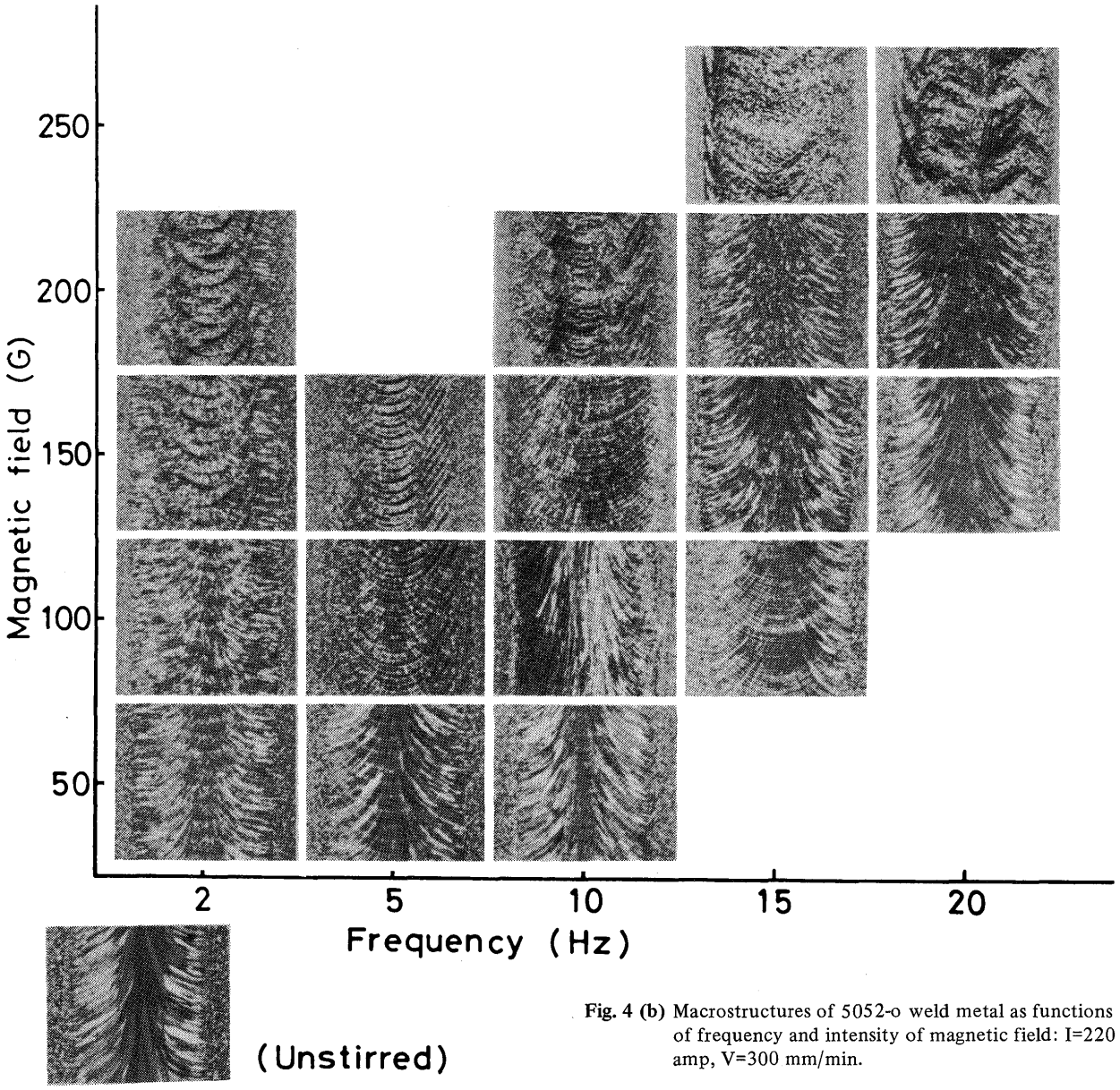

Fig. 4 (b) Macrostructures of 5052-o weld metal as functions of frequency and intensity of magnetic field: I=220 amp, V=300 mm/min.

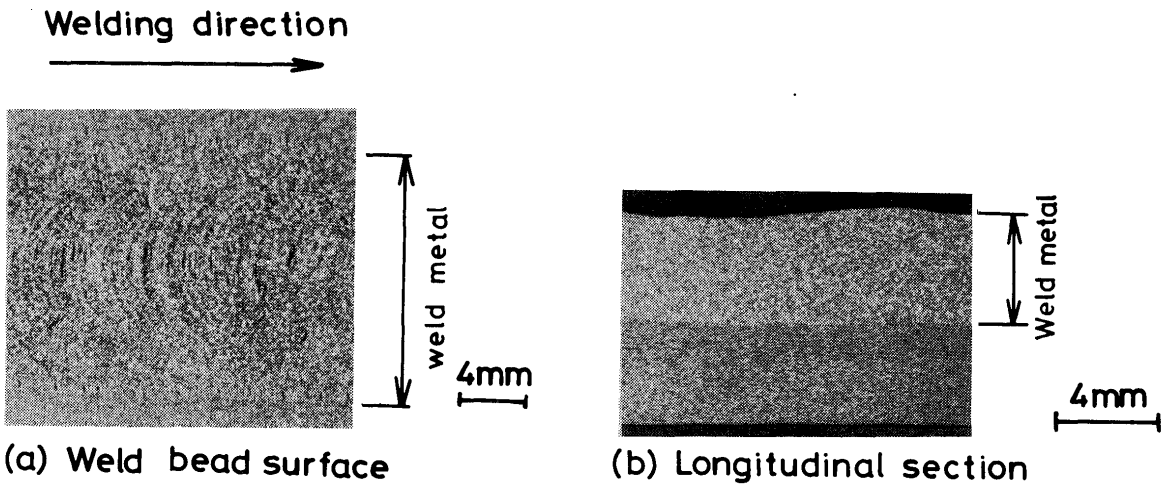

Fig. 5 Macrostructure of weld bead surface and longitudinal section; 5083-o, V=300mm/min, I=220amp, 10Hz, 100G.

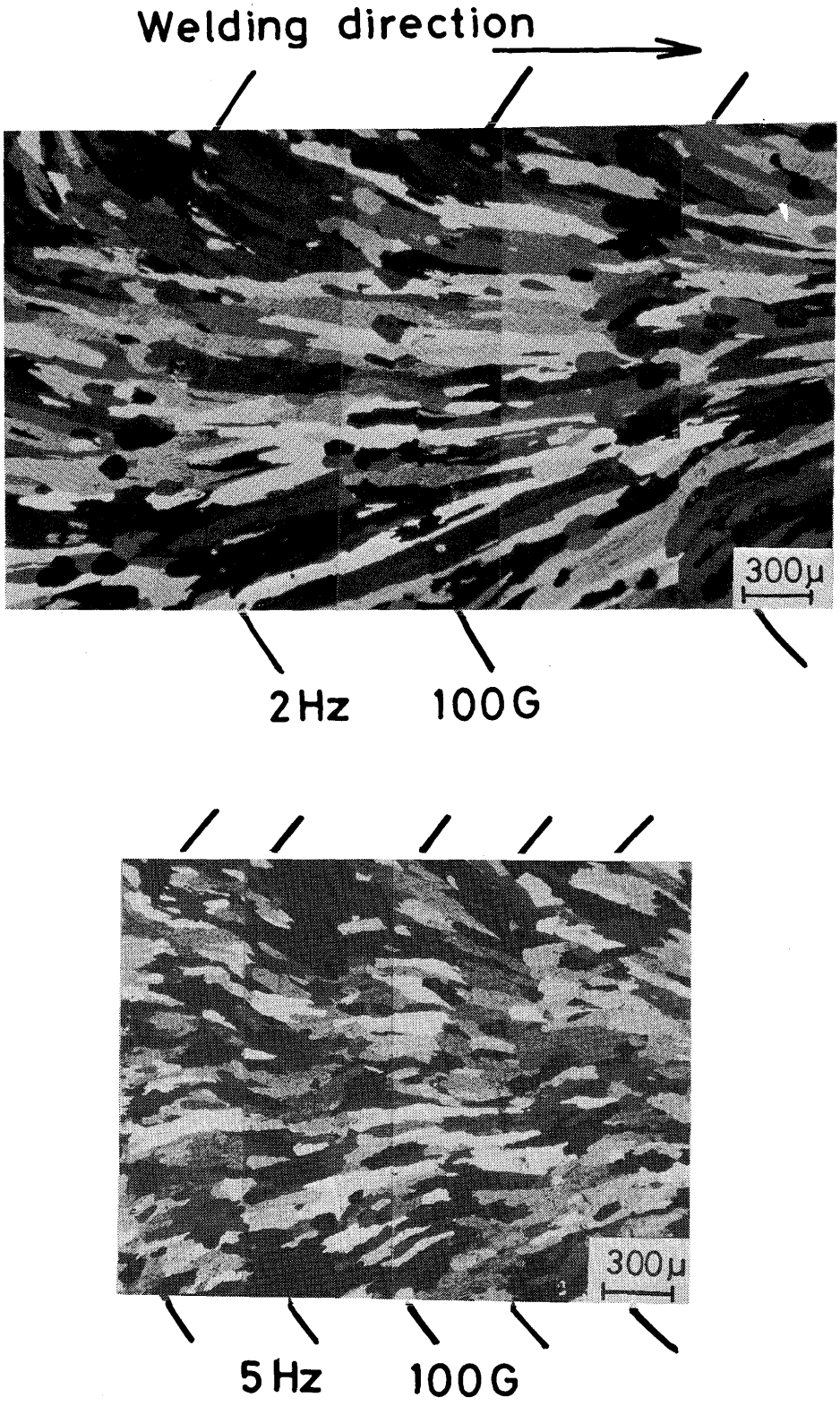

Fig. 6 Effect of frequency of magnetic field on growth period of columnar crystal in weld center. material; 5052-o, V=300mm/min, I=220amp, 100G.

line in the top and bottom of the photograph indicates a ripple line where the porality of the magnetic field was altered. These ripple lines are considered to be formed by the abrupt change of the flow direction of the molten metal due to the change in the polarity of the magnetic field. The distance between two ripple lines corresponds to the distance that the solidification front advances during a half period of the frequency. In Fig. 6, in the case of 2 H_Z the most of the columnar crystals were stopped their growth at each ripple line and the newly nucleated crystals again grow forward as new columnar crystals from the ripple line to the next one. Increasing the frequency to 5 Hz, the columnar crystals decreased their length of growth in accordance with the decrease of the distance between two ripple lines. At the same time the width of them also became narrower. Thus, the grain refinement is the most remarkable in 5 Hz. These abrupt changes in the solidification structure at the ripple line are more clearly shown in **Fig. 7**. A pair of the bold line in Fig. 7 indicates

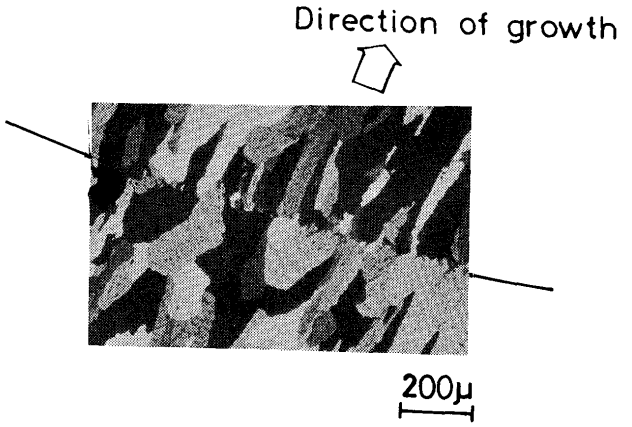

Fig. 7 Occurrence of new crystals at ripple site. material; 5052-o, V=300mm/min, I=220 amp, 5Hz, 100G.

a ripple line. In Fig. 7, many small crystals of those were grown forward suppressing the growth of the columnar crystal reached to this ripple line.

As a result, it has been made clear that for 5052-o, the grain refinement has been performed as the growing length of the columnar crystal along the weld center was almost identical to the distance between two ripples during a half cycle of the alternate magnetic field. These phenomena were almost the same as those observed in the previous report[10] about 2-dimensional GTA (dcrp) weld bead of 2 mm thin sheet of aluminum alloys.

Next, as mentioned in the above 5083-o is much more susceptible for the grain refinement than 5052-o. Therefore, the microstructural change caused by the electromagnetic stirring seems to be considerably different from that of 5052-o as shown macroscopically in Fig. 4. The typical example of the microstructure in the central zone in the weld bead of 5083-o are shown in **Fig. 8** at the various intensity of the magnetic field up to 100 G under a constant frequency of 2 Hz. Each pair of bold line in the right and left of the photograph indicates each ripple line. At the weak intensity as 25 G, the length of the columnar crystal almost corresponds to the distance between two ripple lines and very small crystals are nucleated at these ripple lines. Increasing the intensity to 50 G, the much more grains begin to be nucleated and grow not only at the ripple line but also at the area between two ripple lines, so the grains are fairly refined comparing with those at 25 G and lengths of them become much shorter than those between two ripple lines. Therefore, the grains look like almost the equiaxed crystals. As a result from Fig. 8, it has been made clear that for 5083-o, at the comparably weak intensity of the magnetic field, the grains were refined as the same mechanism as observed in the weld bead of 5052-o that the length of the grain corresponded to the distance between two ripple lines, on the contrary, at the most effective intensity, however, the grains were remarkably refined and the length became much shorter than the distance between two ripple lines. Moreover, the grains were refined to almost the same size as about 100 μ in the central zone of the weld bead even in the various frequencies of 2 to 15 Hz at each optimum intensity. These phenomena were observed independently of the welding speed as 150 and 300 mm/min.

It is considered that the grain refinement by the electromagnetic stirring is mainly due to the fragmentation of the arms of the cellular dendrite. Taking the facts into consideration that at comparably weak intensity, the grain size almost corresponded to the distance between the ripple lines and also the small newly nucleated crystals were observed at each ripple line, it seems that the many small crystals were nucleated at the solidification front at each ripple line, especially around the bottom of the weld bead and then, these newly nucleated small cyrstals were transferred along the advancing solidification front in the weld bead by the flow of the molten metal electromagnetically induced. Further investigation will be continued in future as to the relation between the molten metal flow along the solidification front and the grain refinement.

Next, as to 1070-o, the grain refinement was not observed in this experiment. **Figure 9** shows the microstructure of the weld metal near the ripple line at the condition of 2 Hz and 100 G. The nucleation of the small crystal at the ripple line is not observed and the columnar crystals only varied their growing directions toward for the flowing direction of the molten metal.

It seems that the difference in the susceptibility for the grain refinement of material mostly depended on the

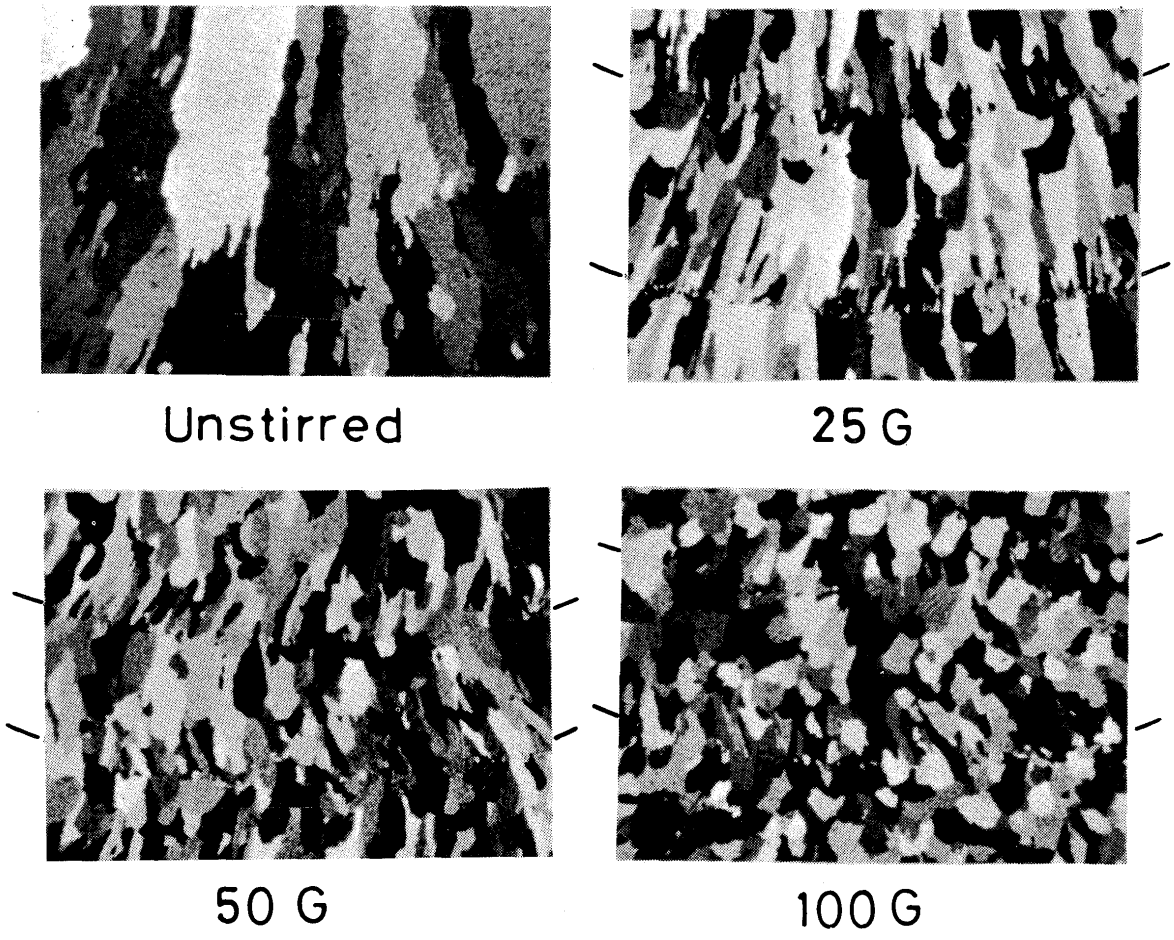

Fig. 8 Effect of intensity of magnetic field on microstructures of 5083-o weld metal. V=150mm/min, I=170amp, 2Hz.

morphology of the growing cellular dendrite. That is, for the material whose amount of alloying element is little such as 1070-o, and the advancing solidification front is almost similar to the plannar interface, the fragmentation of the arms of the cellular dendrite is considered to become more difficult.

3.3 Effect of electromagnetic stirring on elimination of feathery crystal

As pointed out in 3.1, the weld bead of 5083-o is very subject to the formation of the feathery crystal. It has been reported[10] that the electromagnetic stirring is also very effective to suppress the formation of the feathery crystal.

A typical example for the effect of the electromagnetic stirring is shown in **Fig. 10**. The feathery crystal growing from left side to the ripple line indicated by a pair of bold line was completely stopped its growth as soon as the electromagnetic stirring was applied during welding. Then the equiaxed small crystals were formed by stirring in the right hand of the ripple line in Fig. 10. In addition, the relation between the frequency or the intensity of the magnetic field and the formation of the feathery crystal is quantitatively shown in **Fig. 11** for 5083-o. In Fig. 11,

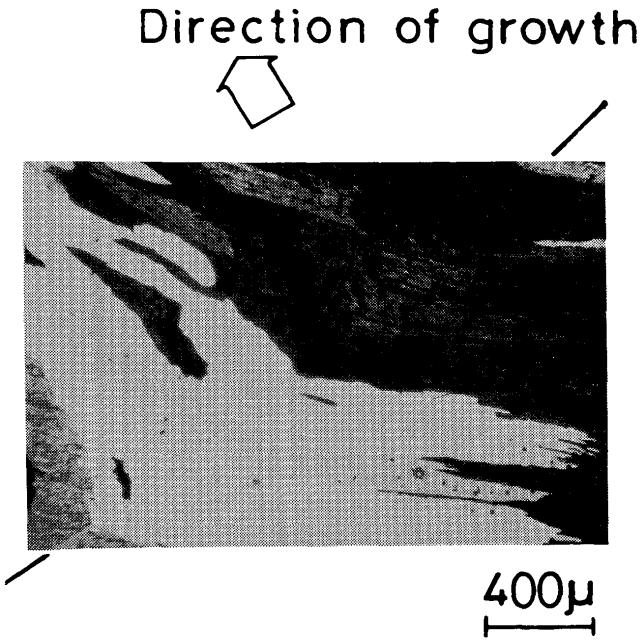

Fig. 9 Microstructure of weld metal near ripple line. material; 1070-o, 2Hz, 100G.

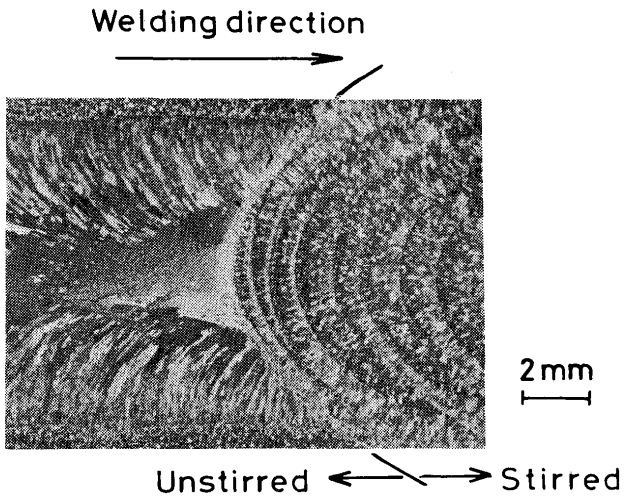

Fig. 10 Extinction of feathery crystal by application of electromagnetic stirring. material; 5083-o, V=300mm/min, I=220amp, 2Hz, 100G.

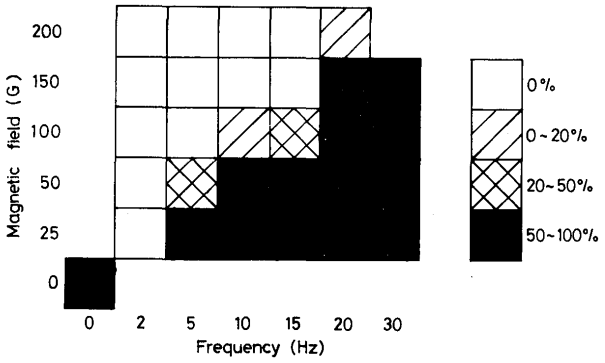

Fig. 11 Effect of frequency and intensity of magnetic field on elimination of feathery crystal. material; 5083-o, V=300mm/min, I=220 amp.

the ratio in percent of the length of the feathery crystal to that of the weld bead is shown as the density of the hatching. In unstirred condition as shown in 0 (G) and 0 (Hz), the feathery crystal was formed at the ratio of 50 to 100%. As regards to the frequency at a constant intensity of 100 G, the effect of the magnetic stirring is the most remarkable at 2 to 5Hz, that is, 0%, but as increasing the frequency this effect decreased, and more than 20 Hz the feathery crystal again formed as many as unstirred. The range of the effective condition of the magnetic field is the widest at low frequencies, especially around 2 Hz and at the higher frequency this range become narrower. This effective range was wider than that for the grain refinement. In order to eliminate the feathery crystals in the weld bead, more than 25 G in 2 Hz, more than 100 G in 5 Hz, more than 100 G in 10 Hz and more than 150 G in 15 Hz were recommended in this experiment.

3.4 Effect of electromagnetic stirring on elimination of porosity

As an another effect of the electromagnetic stirring, it is well known that porosities are decreased in their amount by the electromagnetic stirring[1), 6), 7), 10)]. Therefore, the most effective condition of the electromagnetic stirring for the elimination of porosities has been also examined. The bead-on-plate welding by the GTA in dcsp has been carried out with a mixing gas of He + 0.5% H_2 as a shielding gas for 5083-o under a constant welding condition, that is, 300 mm/min of the welding speed and 220 amp of the welding current. The typical distributions of porosities are shown in **Fig. 12** in the parallel surface to the plate surface in the upper and in the

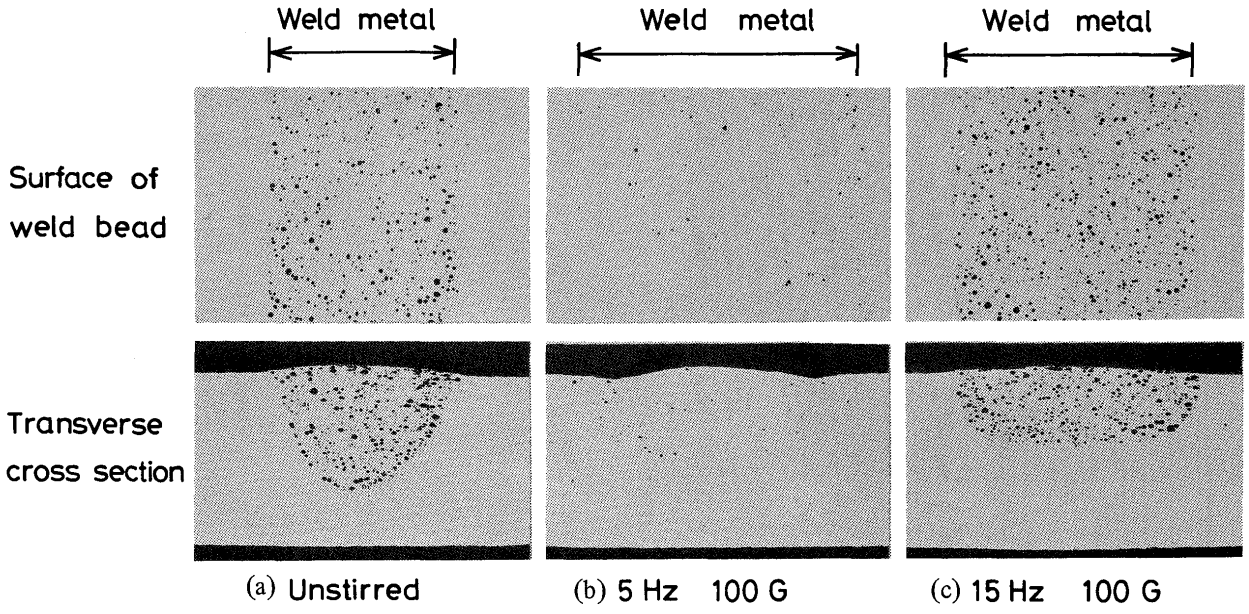

Fig. 12 Effect of electromagnetic stirring on elimination of porosity, (a) Unstirred (b) 5Hz, 100G (c) 15Hz, 100G material; 5083-o, V=300mm/min, I=220amp.

transverse crosssection in the lower without and with the electromagnetic stirring of 5 and 15 Hz for 100 G. In (a) at unstirred condition there are large amount of porosities, especially near the fusion boundary. The distribution along the ripple line was also partly observed. Nextly with electromagnetic stirring of 5 Hz and 100 G as in (b) the amount of them were remarkably decreased, but in the case of 15 Hz as in (c), the effect of the electromagnetic stirring was little and the distribution of porosities was almost the same as that without stirring, though the shape of the fusion zone became shallower and wider due to stirring.

In addition, the microstructure of those porosities have been observed by the scanning electron microscope (SEM). **Figures 13 (a), (b)** and (c) show the typical examples. from Fig. 13 (a), it is apparent that porosities can be classified into two groups due to the difference in the morphology, that is, one is typical blow hole whose appearance is spherical shape as in (b), and the other is like worm hole whose appearance is elongated or irregular shape as in (c). From Fig. 13 (b), the dendritic mode is observed on inner surface of the blow hole, though its surface is comparably flat. On the contrary, as shown in Fig. 13 (c), the distinct dendritic mode is observed on inner surface of the worm hole and this mode is similar to that of fracture surface of solidification crack occurred just below the liquidus[13].

Moreover, in order to quantitatively evaluate the effect of the frequency and the intensity of the magnetic field, the area fraction of porosities has been measured on the bead surface after elimination of the reinforcement by the

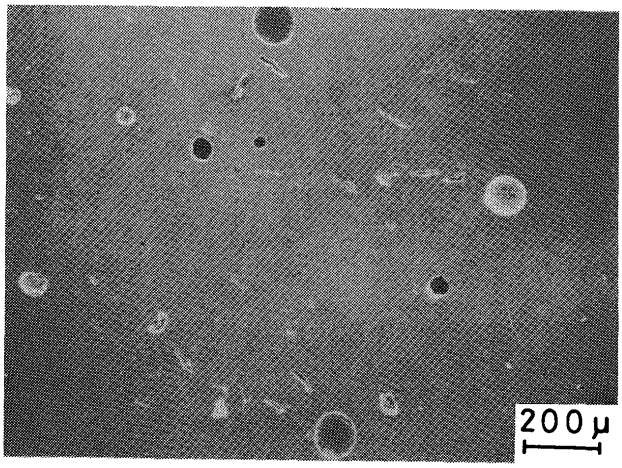

(a) Lower magnification of porosity

Fig. 13 SEM microstructure of porosity in 5083-o weld metal unstirred.

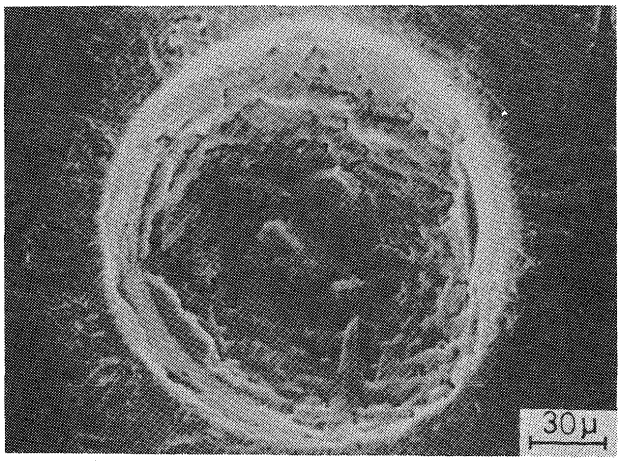

(b) Higher magnification of blow hole

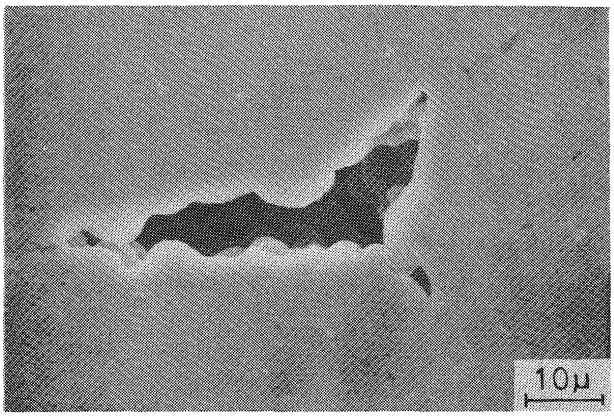

(c) Higher magnification of worm hole

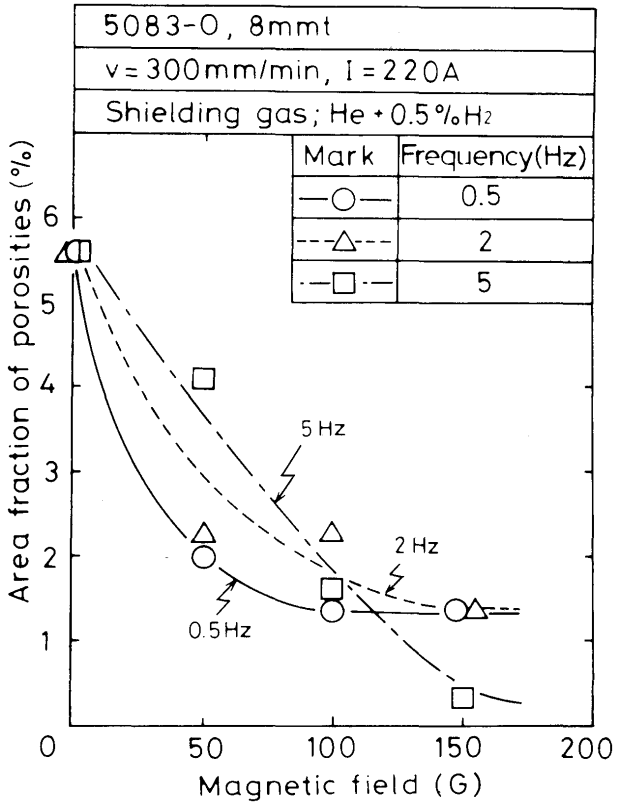

Fig. 14 Relation between intensity of magnetic field and area fraction of porosities.

aid of the point counting method as mentioned in previous report[10]. The results are shown in **Figs. 14** and **15** . As to the effect of the intensity of the magnetic field

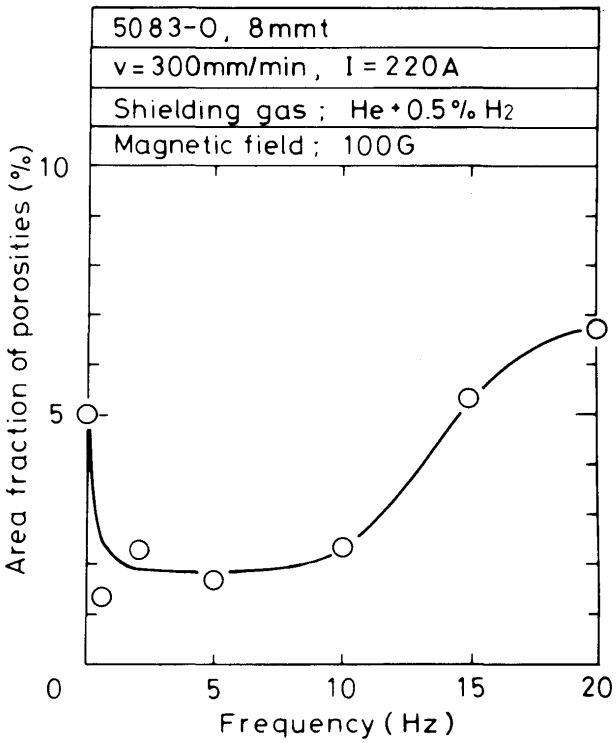

Fig. 15 Relation between frequency of magnetic field and area fraction of porosities.

in Fig. 14, the amount of porosites is decreased at the range of 50 to 150 G in each frequency. Increasing the intensity more than 150 G, the weld bead appearance became very rough. Consequently, the strong intensity will be effective to reduce the amount of porosities but there is a limitation of its intensity owing to undesiarable weld bead appearance. Therefore, taking the weld bead appearance into consideration, the most effective intensity of the magnetic field is considered to be about 100 G in this investigation.

Next, Figure 15 shows the effect of the frequency under a constant intensity of 100 G. The amount of the porosities is the least in the frequencies from 0.5 to 10 Hz. However, the effect of the electromagnetic stirring becomes less effective in the case more than 15 Hz. On the other hand, **Figure 16** shows the relations between the intensity of the magnetic field and the amounts of the blow hole and the worm hole, respectively. In Fig. 16, the amount of the blow hole is remarkably decreased at 50 to 150 G in each frequency and as to the worm hole, it is also decreased at 50 to 150 G, but its amount is very little even without stirring. On the other hand, the number of the worm hole which was much more than that of the blow hole was remarkably decreased. From these results, it seems that the decrease in the amount of porosites is mainly due to the decrease in the amount of the blow hole.

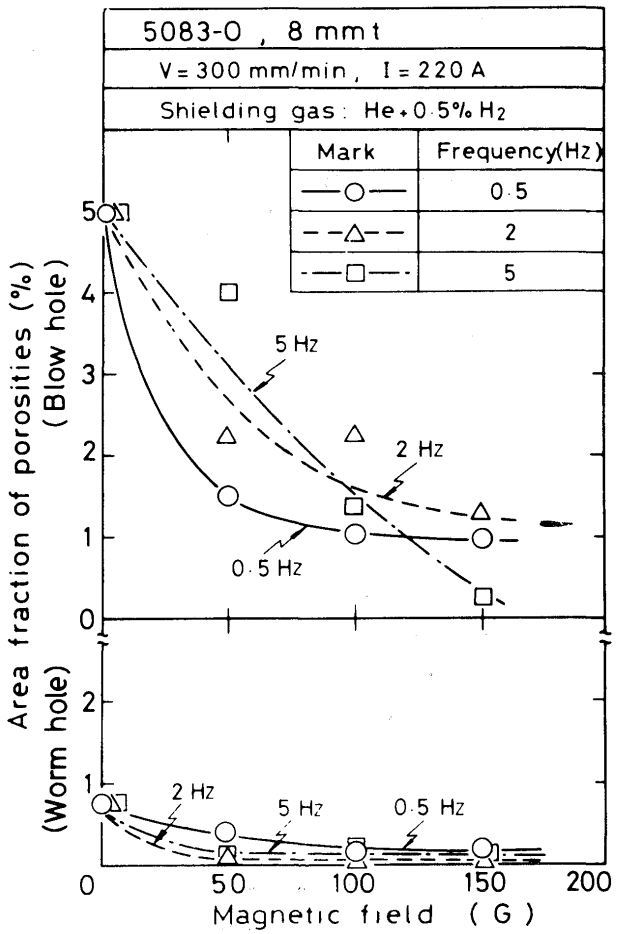

Fig. 16 Relation between intensity of magnetic field and area fraction of porosities.

3.5 Application of electromagnetic stirring for butt welds

In previous sections the fundamental investigations have been carried out for bead-on-plate welding without filler metal. In this section, the electromagnetic stirring has been applied for the butt welding with square groove with filler metal. The materials used is 5083-o which is usually used in the actual welding of large components of aluminum alloys such as the storage tank for LNG. For unstirred welded joint the crosssection of square groove double butt weld beads with filler metal of 5183 (1.6 mm dia.) is shown in **Fig. 17 (a)** and its X-ray radiograph is also shown in **Fig. 17 (b)**. Where, the welding speed; 300 mm/min, welding current; 260 amp and feeding rate of the filler metal; 1050 mm/min. The surface of the groove was removed of grease by the benzine. Some serious defects have been always observed in the butt welds of GTA (dcsp) such as the lack of fusion, large irregular shape worm hole and the well developed feathery crystal as shown in Fig. 17 (a) and (b). In Fig. 17 (a), large irregular shaped worm holes are formed at the

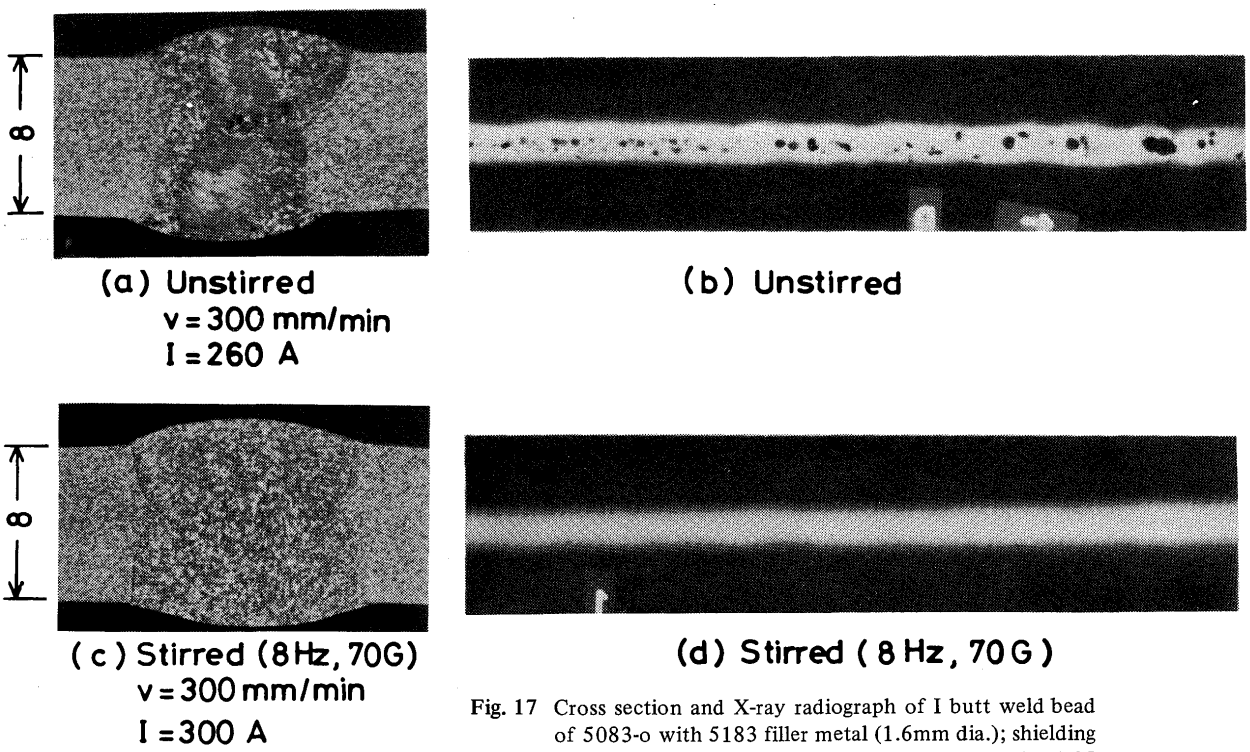

Fig. 17 Cross section and X-ray radiograph of I butt weld bead of 5083-o with 5183 filler metal (1.6mm dia.); shielding gas : H_e, 351/min, Feeding rate of filler metal : 1.05 min.

central zone of the welds. **Figure 18** shows the inner surface of the irregular shaped worm hole which is very rough and seems to be covered with the thick oxide film. These morphology is different from those in the blow hole and worm hole due to H_2 gas in 3.4 where the dendritic mode has clearly observed. The result of the application of the electromagnetic stirring, for an example, in the condition of 8 Hz and 70 G is shown in **Figs. 17 (c)** and **(d)** which show the crosssection and X-ray radiograph of the weld bead, respectively. The welding condition was the same as those unstirred except welding current, which was inceased to 300 amp in order to obtain the same penetration depth because with electromagnetic stirring the penetration depth was generally decreased a little. As a result of comparing Figs. 17 (a) with (c), the irregular shaped worm hole and the feathery crystal are eliminated and also the grain refinement is fully achieved with the electromagnetic stirring. Moreover, the comparison of each X-ray radiograph more clearly shows the effectiveness of the electromagnetic stirring on the suppress of the formation of the irregular shaped worm hole. In Fig. 17 (d), there are no large irregular shaped worm holes except some very little small spherical blow holes.

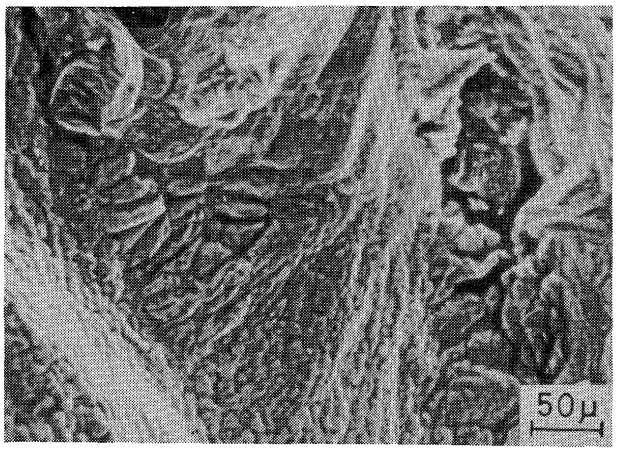

Fig. 18 SEM microstructure of irregular shaped worm hole.

Consequently, it has been apparent that the soundness of the square groove double butt welds by GTA in dcsp could be remarkably increased by the application of the electromagnetic stirring during welding. Another approach may be needed in future, especially, about the arrangement of the magnetic coil and welding torch in order to apply the electromagnetic stirring to the actual welding for industrial purposes.

4. Conclusions

In order to investigate the effect of the electromagnetic stirring of the weld metal on the grain refinement of the solidification structure, the eliminations of the feathery crystal and the porosities, the GTA bead-on-plate welding in dcsp with He gas shielding was carried out for 5083-o, 5052-o and 1070-o aluminum alloys with the electro-

magnetic stirring in the weld pool during welding. Moreover, the application of the electromagnetic stirring to the actual welding process of the square groove double butt welding with filler metal for 5083-o of 8 mm thick plate has been examined.

Main conclusions obtained are as follows;

(1) The effect of the electromagnetic stirring on the grain refinement largely depended on the composition of the material. 5083-o was the most susceptible to the grain refinement and 5052-o was considerably susceptible, but 1070-o was impossible to be refined in this experiment.

(2) There is the most effective frequency of the alternate magnetic field for the grain refinement. For 5083-o, this range of the optimum frequency was wide, which was 2 to 15 Hz at the welding speed of 300 mm/min. On the contrary, for 5052-o, it was comparably narrow, which was restricted around 5 Hz. The strong intensity of the magnetic field is effective to the grain refinement, but there is a limit for the intensity owing to the formation of the unsound rough weld bead surface.

(3) Therefore in order to obtain the grain refinement following optimum conditions for electromagnetic stirring are found out for welding speed of 300 mm/min in this investigation, that is, for 5083-o, 100 to 150 G in 2 Hz, 100 G in 5 and 10 Hz and 150 G in 15 Hz and for 5052-o, 150 G in 5 Hz.

(4) From the result of the observation of the microstructure, in the case of 5052-o the grain refinement has been performed when the growing length of the columnar crystal along the weld center was almost identical to the distance corresponding to the advancing length of the solidification front during a half cycle of the alternate magnetic field. On the contrary, in the case of 5083-o, at the comparably weak intensity of the magnetic field the grain refinement has been performed as the same way as in 5052-o, but at the most effective intensity the grains were remarkably refined and those sizes were much shorter than the length corresponding to a half cycle of the magnetic field.

(5) The feathery crystal was very often observed in the GTA (dcsp) bead-on-plate weld bead for 5083-o at the welding speed of 150 to 1000 mm/min. The formation of this feathery crystal can be easily eliminated with the electromagnetic stirring of molten metal during welding. Considering the surface appearance of the weld bead the optimum conditions were 25 to 150 G in 2 Hz, 100 G in 5 Hz and 150 G in 10 and 15 Hz for 5083-o in this experiment.

(6) The magnetic stirring is effective to reducing the formation of porosities, but there are optimum values for the frequency and the intensity of the magnetic field. The optimum conditions were 50 to 150 G in 0.5 to 10 Hz for 5083-o in this experiment. The excess high frequency decreases its effect.

(7) The electromagnetic stirring remarkably increased the soundness of the GTA (dcsp) butt weld bead of 5083-o with filler metal by almost completely suppressing the formation of the large irregular shaped worm hole and the feathery crystal and also remarkably refined the grains.

Acknowledgement

The authors would like to thank Dr. Masao Ushio, associate professor of JWRI and Dr. Hiroji Nakagawa, research instructor of JWRI, for their kind suggestions and discussions.

References

1) D.C. Brown, F.A. Crossley, J.F. Rudy and H. Schwartzart: Weld.J., Vol. 41 (1962), 241s.
2) H. Shibata and K. Asai: Priprint of the National Meeting of JWS, No. 10 (1972), pp. 231 (in Japanese).
3) H. Shibata and K. Asai: J. JWS, Vol. 41 (1972), No. 7, pp. 811 – 817 (in Japanese).
4) V.A. Blinkov: Svar. Proiz., 1975, No. 11, pp. 11 – 12.
5) E.V. BARDOKIN et al: Svar. Proiz., 1975, No. 11, pp. 12 – 14.
6) O.M.NOVIKOV et al: Svar. Proiz., 1975, No. 11, pp. 14 – 15.
7) V.P. CHERNYSH, V.V. SYROVATKA: Avt. Svarka., 1972, No. 11, pp. 16 – 19.
8) W.H.S. Lawson and H.W. Kerr: Welding Research International, Vol. 6 (1976), No. 5, pp. 63 – 77.
9) W.H.S. Lawson and H.W. Kerr: Welding Research International, Vol. 6 (1976), No. 6, pp. 1-17.
10) F. MATSUDA, H. NAKAGAWA, K. NAKATA and R. AYANI: Trans. JWRI, Vol. 7 (1978), No. 1, pp. 111 – 127.
11) Welding Handbook, JWS, 1977, pp. 1046 (in Japanese).
12) H. NAKAGAWA, M. KATOH, F. MATSUDA and T. SENDA : Trans. JWS, Vol. 3 (1972), No. 2, pp. 54 – 63.
13) Y. ARATA, F. MATSUDA, K. NAKATA and I. SASAKI: Trans. JWRI, Vol. 5 (1976), No. 2, pp. 53 – 67.